International Journal of Minerals, Metallurgy and Materials
Volume 26, Number 2, February 2019, Page 152
https://doi.org/10.1007/s12613-019-1719-7

Effect of reductant type on the embedding direct reduction of beach titanomagnetite concentrate

Yong-qiang Zhao[1,2], *Ti-chang Sun*[1,2], *Hong-yu Zhao*[1,2], *Chao Chen*[1,2], *and Xiao-ping Wang*[1,2]

1) Key Laboratory for High-Efficient Mining and Safety of Metal Mines, Ministry of Education, University of Science and Technology Beijing, Beijing 100083, China
2) School of Civil and Resource Engineering, University of Science and Technology Beijing, Beijing 100083, China
(Received: 27 March 2018; revised: 12 June 2018; accepted: 15 June 2018)

Abstract: Iron and titanium were recovered from beach titanomagnetite (TTM) concentrate by embedding direct reduction and magnetic separation. The reduction products and the effects of the reductant type and reduction temperature on the reduction behavior were investigated. The results showed that the reduction of TTM concentrate was strongly related to the gasification reactivity of the reductant. Bitumite presented a better product index than wheat-straw biochar and coke, mainly because the gasification reactivity of bitumite was better than that of the other reductants. In addition, high temperatures were not beneficial to embedding direct reduction because of the emergence of a molten phase and iron-joined crystals, which in turn reduced the diffusion rate of the reducing gas and impeded the reduction reaction in the central area of the roasted briquette. The use of bitumite as the reductant at a C/Fe molar ratio of 1.4 and a reduction temperature of 1200°C for 120 min resulted in direct-reduction iron powder assaying 90.28wt% TFe and 0.91wt% TiO_2 with an iron recovery of 91.83% and titanium concentrate assaying 46.01wt% TiO_2 with a TiO_2 recovery of 91.19%. Titanium existed mainly in the form of anosovite and ilmenite in the titanium concentrate.

Keywords: beach titanomagnetite concentrate; embedding direct reduction; magnetic separation; reductant; reduction temperature

1. Introduction

Currently, ilmenite is the main resource for the production of metallic titanium and titanium-containing compounds [1–2]. Meanwhile, the demand for titanium dioxides, which are widely used in the paint, paper, and plastics industries, is increasing rapidly [3]. With the continuous depletion of high-grade titanium ores and increasing demand for titanium dioxides, low-grade titanomagnetite (TTM), such as beach TTM ore, has become an important resource [4–5]. Beach TTM, which usually contains 30wt%–66wt% TFe and 6wt%–13wt% TiO_2, has the advantages of large scale reserves, easy mining, and low treatment costs [6–8]. However, TTM concentrate of sufficient quality is difficult to obtain by conventional mineral processing methods because of its fine grain size and complex mineral composition [9], and low-grade TTM concentrate is difficult to use in iron and steel making and titanium smelting [10]. Therefore, the development of an effective method to recover iron and titanium from beach TTM is currently an active research topic.

Some new processes such as the hydrometallurgical processing route [11] and the acid leaching and solvent extraction processes [12–13] have recently been investigated for the recovery of iron and titanium from beach TTM. To some extent, these methods achieve separation of iron and titanium; however, they suffer several disadvantages, including low recovery rates of titanium, relatively high costs, and generation of environmental pollutants [11,13]. Recent research has shown that recovering iron from TTM ore by coal-based direct reduction followed by magnetic separation is feasible [14–17]. Wang *et al.* [18] obtained a magnetic concentrate with 88.4wt% iron content and 92.8% iron recovery from chromium–vanadium-bearing TTM concentrate at a roasting temperature of 1200°C and a roasting time of 60 min. Gao *et al.* [15] reported on recovering iron from Indonesian beach TTM ore by coal-based reduction, and a high grade of direct-reduction iron powder (DRIP) with an iron

Corresponding authors: Ti-chang Sun E-mail: suntc@ces.ustb.edu.cn; Hong-yu Zhao E-mail: yuyu_3003@126.com

content of 93.74wt%, an iron recovery of 95.91%, and a TiO_2 content of 0.45wt%, was obtained. This product can be used as a scrap substitute for steelmaking in electric arc furnaces.

Although the effective recovery of iron was achieved by the aforementioned methods, recovery and rational utilization of the titanium components was difficult, as indicated by assays of the nonmagnetic products showing only 20wt%−30wt% TiO_2. In coal-based direct reduction, when high dosages of the coal and additive (~20wt% and 10wt%, respectively) were added, coal ash and most additives tended to fall into the nonmagnetic product after direct reduction and magnetic separation, thereby leading to poor TiO_2 grades, complex structures, and various titanium minerals in the nonmagnetic products [16]. Therefore, mixing of coal, additives, and TTM is disadvantageous to obtaining a high-grade titanium product.

To efficiently and comprehensively utilize TTM ore, Geng *et al.* [16] have proposed a new process for recovering iron and titanium. In this process, beach TTM concentrate and a binder are initially pelletized and then embedded into coal to avoid the impact of coal ash. The roasted pellets are subsequently separated by magnetic separation to obtain the DRIP and titanium concentrate. Although a few researchers have used this embedding direct reduction process, information about the reductant type and reduction temperature is limited, and how to increase the TiO_2 content in the titanium concentrate has been an issue. In this study, the influences of reductant type and reduction temperature on the embedding direct reduction behavior of TTM concentrate are investigated.

2. Experimental

2.1. Materials

The beach TTM ore was obtained from the Indonesian coast. After drying, the ore was ground to 95wt% passing 0.074 mm. The TTM concentrate used in this study was then obtained using low-intensity magnetic separation at a magnetic field intensity of 80 kA/m. The mineralogical analysis of the beach TTM concentrate was carried out by X-ray diffraction (XRD). The XRD pattern in Fig. 1 indicates that the TTM concentrate consists mostly of TTM ($Fe_{2.75}Ti_{0.25}O_4$), with small amounts of ilmenite ($FeTiO_3$) and quartz (SiO_2). The TTM concentrate contained 57.29wt% TFe and 11.42wt% TiO_2 by assay. Details of the TTM concentrate are described in a previous paper [16].

Bitumite, wheat-straw biochar (WS-char), and coke were collected from Yuzhou city, Henan province, China. The samples were cut to the sizes of 0.5–1.0 mm. The industrial analysis results for the reductant are shown in Table 1. To study the effect of gasification reactivity of the reductant on the embedding direct reduction process, bitumite was devolatilized in a fixed-bed reactor under a flowing nitrogen atmosphere at a temperature of 900°C for 60 min. The reactivity tests were then conducted under a CO_2 atmosphere on a thermogravimetric analyzer. The gasification reactivity test methods are described in a previous paper [19]. As shown in Fig. 2, gasification reactivity of bitumite char is slightly better than that of WS-char. In addition, gasification reactivity of coke is the worst.

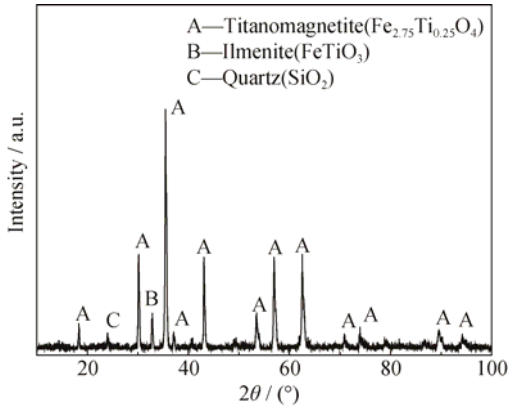

Fig. 1. XRD pattern of the beach titanomagnetite concentrate.

Table 1. Industrial analysis results for the reductant used in the experiments wt%

Reductant	Fixed carbon	Volatiles	Moisture	Ash
Bitumite	56.66	29.54	7.25	6.55
WS-char	80.12	6.26	9.82	3.80
Coke	80.80	2.66	1.18	15.36

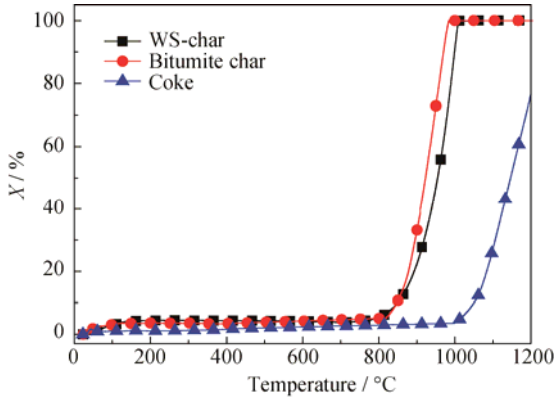

Fig. 2. Gasification conversion curves of different chars.

The gasification conversion (X) was calculated using the following equation:

$$X = \frac{m_0 - m_t}{m_0 - m_{ash}} \times 100\% ,$$

where m_0 denotes the sample mass at the start of gasification; m_t is the sample mass at gasification time t; and m_{ash} is the mass of ash remaining in the sample.

2.2. Experimental procedures

The wet briquettes were prepared by mixing the TTM concentrate with 0.5wt% binder and a certain amount of water in an experimental disk pelletizer. The wet briquettes of 12.5–13.5 mm in diameter were then dried at 105°C for 5 h to remove free moisture. After the briquettes were dried, 25 g of dry briquettes was embedded in excessive reductant (C/Fe molar ratio of 1.4). The embedded briquettes were then placed in a graphite crucible with a lid, and the crucible was placed inside a furnace. The crucible charging method is shown in Fig. 3. The furnace was heated to a predetermined temperature with an adequate holding time (120 min). The crucible was then removed from the furnace and cooled naturally to room temperature. The reduced briquettes were ground, and then separated in a magnetic tube. The grinding experiments were conducted in a rod mill (RK/BM-1.0L) with 10 rods (ϕ15 mm × 120 mm) at 66.6wt% solid density and with a speed of 289 r/min. The first-stage grinding time was 20 min. A magnetic field intensity of 144 kA/m was used to separate metallic iron from the slurry. After that, the iron concentrates obtained from the first separation were reground for 25 min, and then they were magnetically separated with a magnetic field intensity of 144 kA/m. The final iron concentrate and mixed nonmagnetic product are referred to as DRIP and titanium concentrate, respectively. The iron content, iron recovery, and TiO_2 content in the DRIP, the TiO_2 content, and the TiO_2 recovery in the titanium concentrate were used to assess the product index.

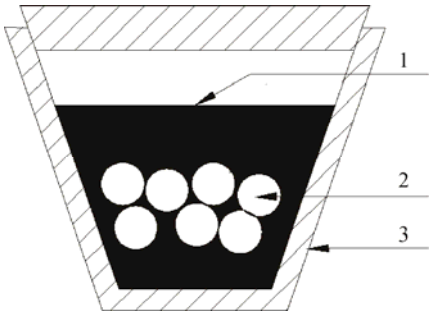

Fig. 3. Crucible charging method. 1—Reductant; 2—Briquettes; 3—Crucible.

2.3. Analysis and characterization

The chemical compositions of the sample were examined by inductively coupled plasma atomic emission spectrometry (ICP-AES, Optima 5300DV, PerkinElmer, USA). Scanning electron microscopy (SEM) with energy-dispersive spectroscopy (EDS, EVO18, Carl Zeiss, Japan) analysis was performed on reduced briquettes mounted on epoxy resin and subsequently polished and sprayed with carbon. Phases present in the samples were identified by XRD carried out on a Rigaku DMAX-RB X-ray diffractometer equipped with a Cu target. The concentrations of CO and CO_2 in the reaction process were detected with an infrared flue gas analyzer (MRU Messgeräte für Rauchgase und Umweltschutz GmbH, Neckarsulm, Germany).

3. Results and discussion

3.1. Effect of reduction temperature

3.1.1. Magnetic separation

The experimental conditions were a roasting time of 120 min, a C/Fe molar ratio of 1.4, and bitumite as the reductant. The effects of reduction temperature on the reduction–magnetic separation were investigated.

As shown in Fig. 4(a), the reduction temperature clearly influenced the DRIP index. When the roasting temperature was increased from 1200 to 1300°C, the iron content of the DRIP increased from 90.28wt% to 93.87wt%; however, the iron content decreased when the temperature was increased further. The iron recovery of the DRIP decreased with increasing temperature, whereas the TiO_2 content of the DRIP first decreased slightly and then increased as the roasting temperature was increased from 1200 to 1400°C. As shown in Fig. 4(b), as the temperature increased from 1200 to 1400°C, the TiO_2 content of the titanium concentrate decreased substantially from 46.01wt% to 36.54wt%, whereas the TiO_2 recovery of titanium concentrate initially increased from 91.19% to 94.29% and then decreased to 90.24%. These results reveal that increasing the roasting temperature adversely affected the Fe recovery of the DRIP and the TiO_2 content of the titanium concentrate. In the previous reports, a high reduction temperature was found to be conducive to coal-based direct reduction [6,20]. By contrast, in this paper, the effect of high temperature on embedding direct reduction is the opposite. To fully explain the experimental data, briquettes roasted at different temperatures were characterized by XRD.

3.1.2. Phase transformation

Fig. 5 shows the XRD patterns of the briquettes roasted at different reduction temperatures. The dominant iron phase is metallic iron, and the majority of titanium exists in the form of anosovite in the sample roasted at 1200°C. When the reduction temperature increases to 1300°C, new phases of wustite, ilmenite, and TTM are observed, which suggests that the reduction atmosphere was insufficient, resulting in

inhibited reduction of the TTM concentrate. The briquettes roasted at 1400°C contain metallic iron, ilmenite, anosovite, and TTM. TTM, in particular, is a titanium mineral with a high iron grade and a poor TiO_2 grade, which can result in low-grade TiO_2 in the titanium concentrate and low iron recovery in the DRIP after magnetic separation. To fully explain the experimental results and to further explore the reduction mechanism, samples roasted at different reduction temperatures were studied by SEM.

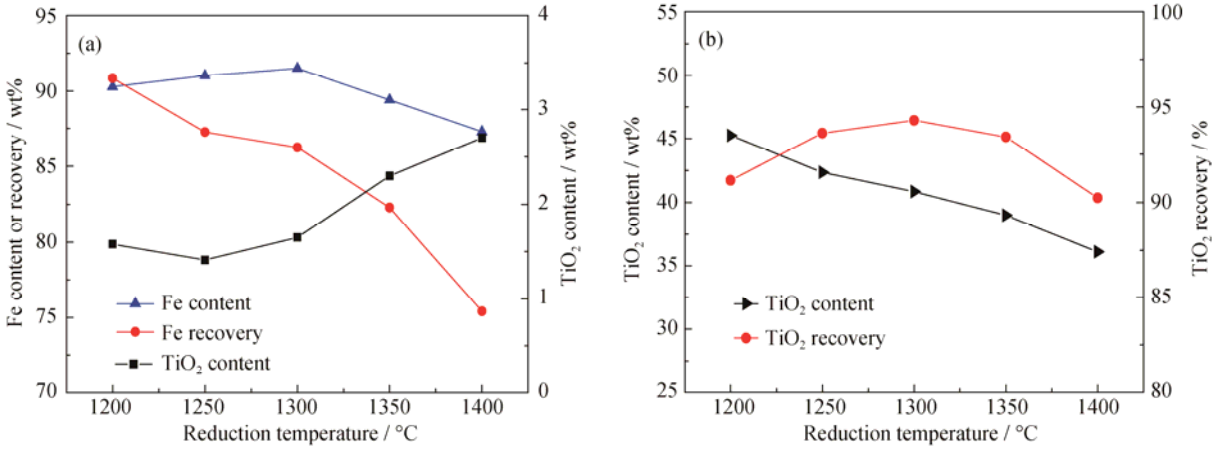

Fig. 4. Effect of reduction temperature on the reduction–magnetic separation: (a) DRIP; (b) titanium concentrate.

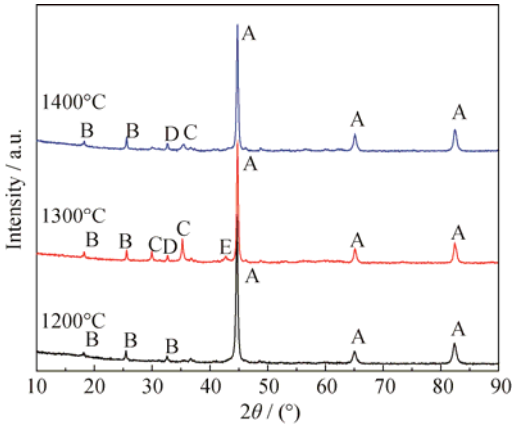

Fig. 5. XRD patterns of briquettes roasted at different reduction temperatures. A—Iron (Fe); B—Anosovite ($(Fe,Mg)Ti_2O_5$); C—Titanomagnetite ($Fe_{2.75}Ti_{0.25}O_4$); D—Ilmenite ($FeTiO_3$); E—Wustite (FeO).

3.1.3. Morphological analysis

The microstructures of the roasted samples were analyzed by SEM coupled with EDS. As shown in Figs. 6(b) and 6(c), the main minerals in the sample roasted at 1200°C are metallic iron and anosovite. In addition, many pore structures exist in the briquettes, which is beneficial to the diffusion of the reducing gas. In the sample roasted at 1300°C, the main minerals are metallic iron and anosovite in the edge area (Fig. 6(e)). In addition, the iron particles become bigger, extensively interconnect, and form iron-joined crystals, resulting in a bright-white ring in region j of Fig. 6(d), which could decrease the efficiency of gas diffusion. This effect may explain why some unreduced TTM and wustite are observed in the central area in Fig. 6(f). When the temperature is increased to 1400°C, the iron particles aggregate further to form particles larger than 80 μm with a plate structure, and the reduced briquette surface is saponaceous, which illustrates that the briquette was molten during the reduction process, as shown in Fig. 6(h). In addition, some titanium-bearing minerals are enwrapped by metallic iron and some unreduced TTM is found in the central area in the sample roasted at 1400°C. These phenomena indicate that the magnetic separation of iron and titanium in the sample roasted at 1400°C will be difficult. Therefore, the roasting temperature was fixed at 1200°C in the subsequent experiment.

3.2. Effect of reductant type

3.2.1. Magnetic separation

The effect of reductant type on the reduction–magnetic separation was investigated. The experiments were performed at a roasting temperature of 1200°C, a roasting time of 120 min, and a C/Fe molar ratio of 1.4. Fig. 7(a) shows that, when bitumite is used as the reductant, the iron recovery and the iron content are the highest and the TiO_2 content of the DRIP is the lowest. Fig. 7(b) shows the effect of reductant type on the titanium concentrate index. Bitumite clearly presented better product index compared with wheat-straw biochar or coke. The DRIP (assaying 90.28wt% TFe and 0.91wt% TiO_2 with an iron recovery of 91.83%) and the titanium concentrate (assaying 46.01wt% TiO_2 with

a TiO_2 recovery of 91.19%) were obtained when bitumite was used as the reductant.

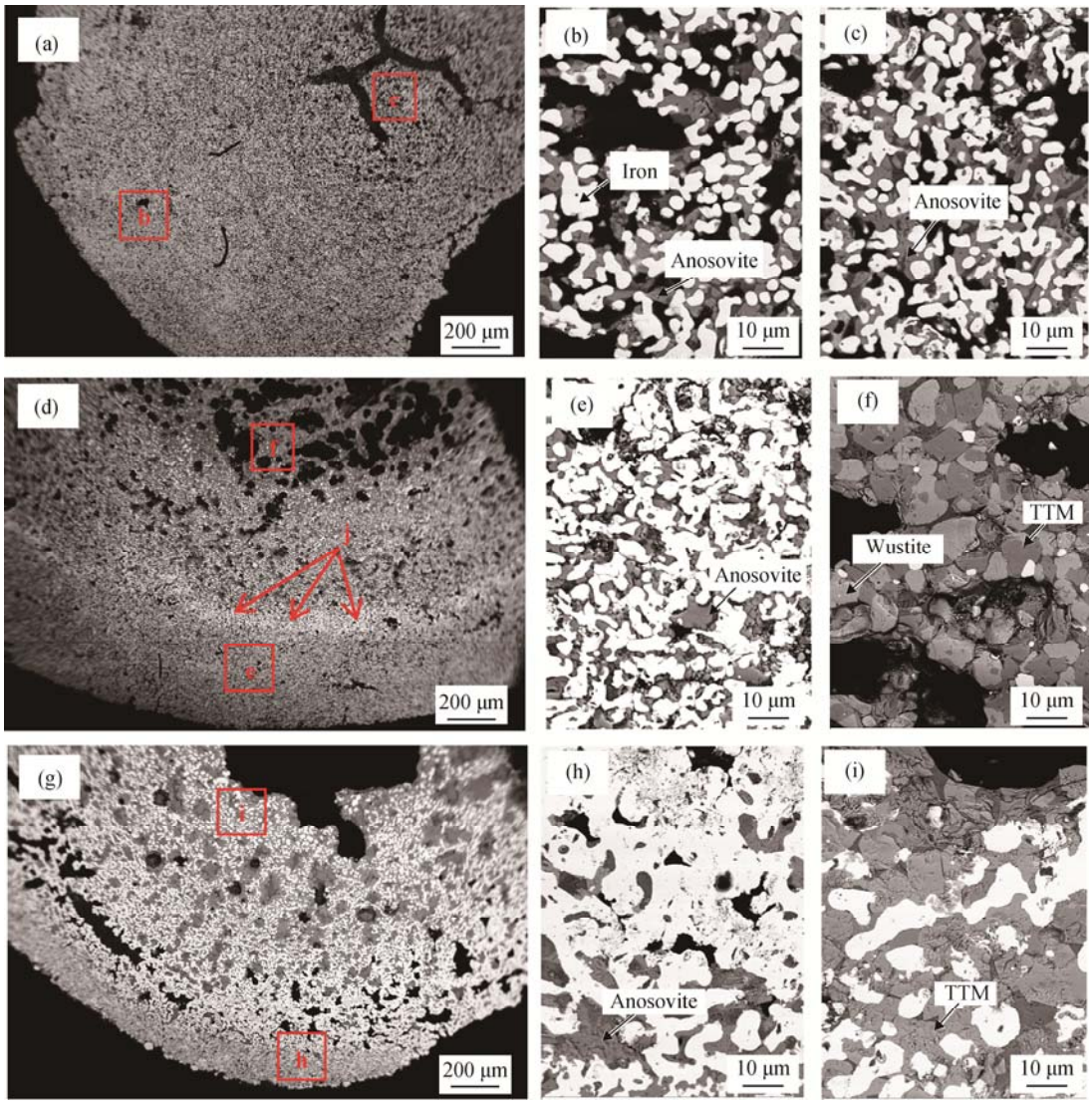

Fig. 6. SEM images of samples roasted at different reduction temperatures: (a–c) 1200°C; (d–f) 1300°C; (g–i) 1400°C.

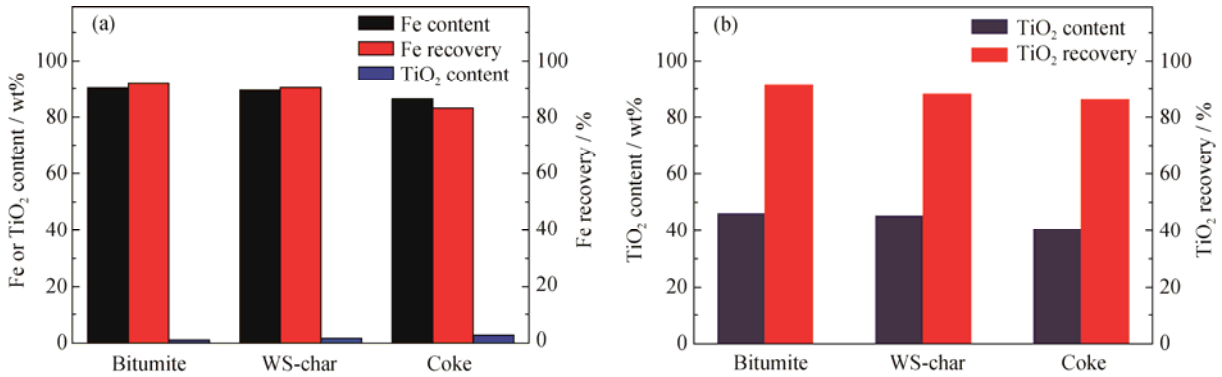

Fig. 7. Effect of reductant type on the reduction–magnetic separation: (a) DRIP; (b) titanium concentrate.

3.2.2. Phase transformation

As shown in Fig. 8, when bitumite is used as the reductant, the dominant phases are metallic iron and anosovite. No new phase is observed when WS-char is used as reductant.

However, when coke is used as the reductant, wustite and TTM are observed and the intensity of the metallic iron diffraction peaks decreases slightly, suggesting that the reducing atmosphere was insufficient during the reduction process. In this study, because the briquettes are embedded in the reductant, the reduction process of TTM briquettes mainly occurs from outside to inside and the carbothermal reduction atmosphere of TTM briquettes may be mainly controlled by the gasification of the reductant, i.e., the Boudouard reaction. On the basis of the analyses in Fig. 2, the reactivity testing results show that gasification reactivity of bitumite char is better than that of WS-char and the gasification reactivity of coke is the worst. The results show that the reduction of TTM concentrate is strongly related to the gasification reactivity of the reductant.

3.2.3. Morphological and gas analysis

When WS-char is used as the reductant, pore structures exist in the briquettes and the main minerals are metallic iron and anosovite. However, metallic iron and anosovite do not exhibit an obvious boundary and some metallic iron is enwrapped by anosovite, which will adversely affect the separation of iron and titanium. When coke is used as reductant, a bright-white ring (region g in Fig. 9(d)) is observed and some unreduced TTM and wustite are found in the central area (Fig. 6(f)), suggesting that the reducing atmosphere was insufficient. The combination of these results with those of a previous report [21] indicates that, if the reducing atmosphere was too weak, large amounts of low-melting materials would be easily formed. Consequently, newly generated iron particles diffused and aggregated more freely and the particles gradually connected to each other. Finally a layer of iron shell was formed inside the roasted briquette during the reduction process, which in turn led to severe deterioration of the reduction reaction in the central area.

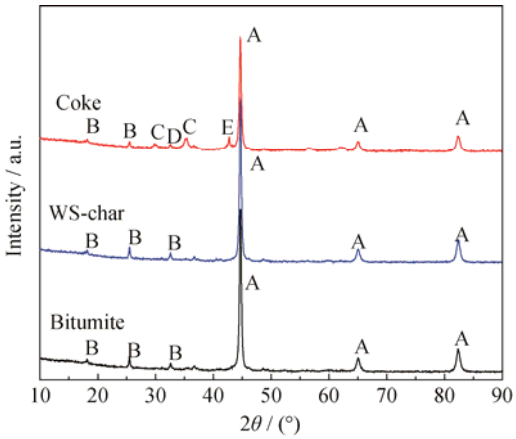

Fig. 8. XRD patterns of briquettes roasted with different reductants. A—Iron (Fe); B—Anosovite (Fe, Mg)Ti_2O_5; C—Titanomagnetite ($Fe_{2.75}Ti_{0.25}O_4$); D—Ilmenite ($FeTiO_3$); E—Wustite (FeO).

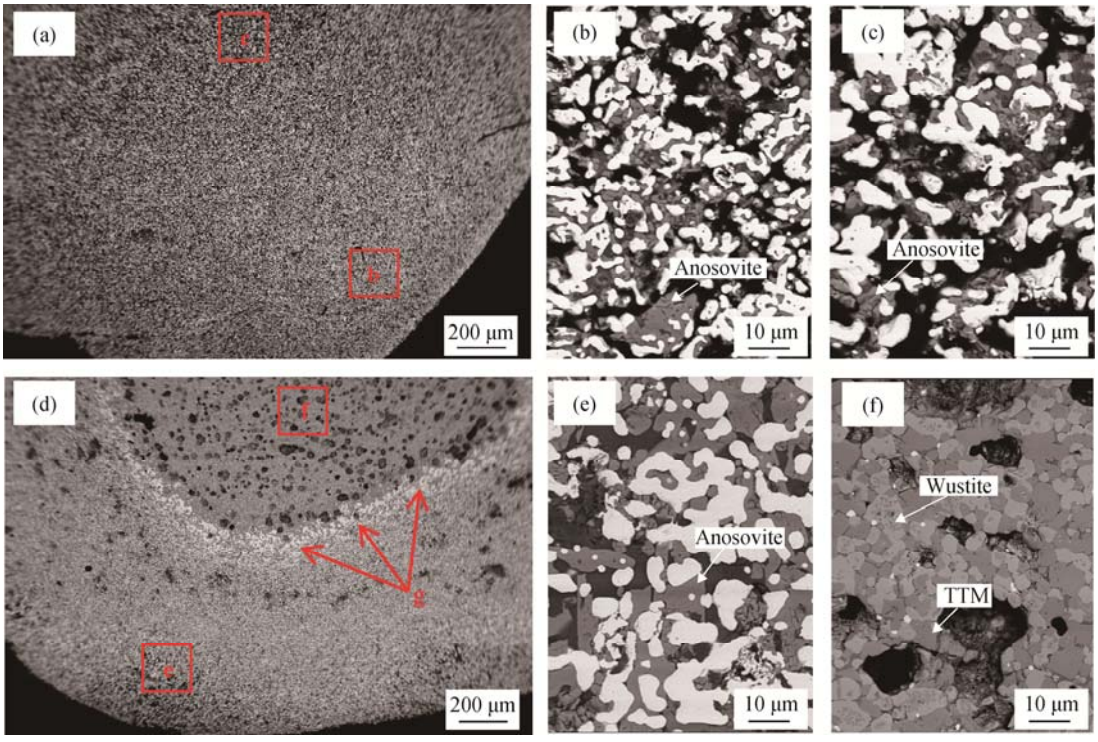

Fig. 9. SEM images of briquettes roasted with different reductants: (a–c) WS-char; (d–f) coke.

Clarifying the mechanism of reduction of the TTM concentrate requires measurements of the concentration changes of CO and CO_2 during the reduction process. Because the gaseous reduction of TTM and the Boudouard reaction of carbon proceed in parallel and affect each other through the concentration changes of CO and CO_2 [22], it was attempted to plot the compositional change of CO in the mixture of CO and CO_2 obtained at a roasting temperature of 1200°C and a C/Fe molar ratio of 1.4.

As shown in Fig. 10, two peaks are observed when bitumite is used as the reductant. The first peak is mainly due to the release of volatile matter in the roasting temperature range from 400 to 500°C. The $CO/(CO + CO_2)$ volume ratio then rapidly rises to the second peak, mainly because of the gasification of char, i.e., the Boudouard reaction. Finally, the $CO/(CO + CO_2)$ volume ratio decreases and then reaches a steady state, which suggests that the reduction of the TTM concentrate tends to end. When WS-char or coke is used as the reductant, only one peak is observed. In addition, the initial reaction time of the reductant clearly differs and the carbothermal reduction reaction of bitumite occurs much earlier, which may be more beneficial to the gas–solid reaction. For example, for the reduction of wustite to metallic iron, the $CO/(CO + CO_2)$ volume value should be greater than 60% [23]; because the gasification reactivity of bitumite char is higher than that of the other reductants, the $CO/(CO + CO_2)$ volume ratio can be greater than 60% at lower temperatures and the reaction would proceed much earlier. Coke, which exhibits the lowest reactivity among the three investigated reductants, will react at higher temperatures. However, higher temperatures are beneficial to forming a molten phase and wustite will become easier to react with gangue to generate large amounts of low-melting material. As a result, the gas–solid reaction is inhibited at higher temperatures [21,24].

3.3. Sample characteristics

The mineral compositions of DRIP and titanium concentrate were determined under the optimum conditions, which were reduced at 1200°C for 120 min with bitumite as the reductant and a C/Fe molar ratio of 1.4. As shown in Fig. 11, the main mineral of DRIP was metallic iron; titanium existed mainly in the form of anosovite and ilmenite in the titanium concentrate. Moreover, the main chemical compositions of the final reduced product were evaluated and are shown in Table 2.

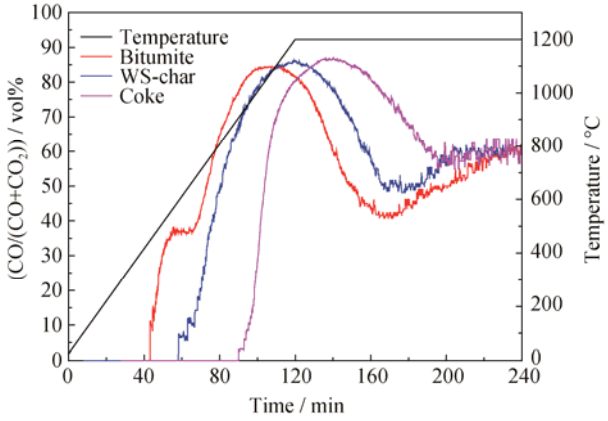

Fig. 10. Effect of reductant type on $CO/(CO + CO_2)$ volume ratio.

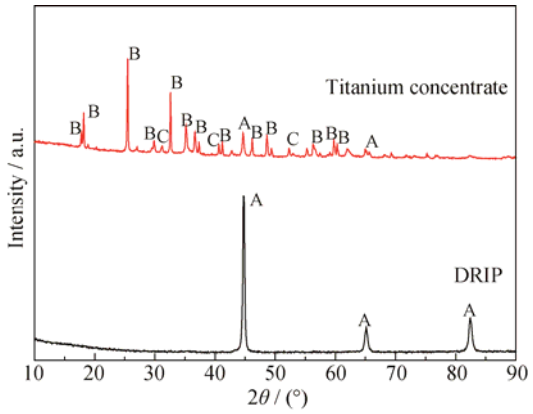

Fig. 11. XRD patterns of DRIP and titanium concentrate. A—Iron (Fe); B—Anosovite $(Fe,Mg)Ti_2O_5$; C—Ilmenite $(FeTiO_3)$.

Table 2. Main chemical compositions of the obtained samples wt%

Sample	Fe	TiO_2	SiO_2	Al_2O_3	MgO	CaO	MnO	Na_2O	P	S	C
DRIP	90.28	0.91	2.31	1.94	1.28	0.42	0.49	0.07	0.05	0.07	0.16
Titanium concentrate	20.70	46.01	10.37	5.23	5.96	0.87	1.13	0.11	0.03	0.14	—

4. Conclusions

(1) In the embedding reduction process, the reduction of roasted briquettes is strongly related to the gasification reactivity of the reductant. Because the gasification reactivity of bitumite char is better than those of wheat-straw biochar and

coke, carbothermal reduction reactions of bitumite occur earlier and at lower temperatures, which is beneficial to inhibiting the generation of low-melting materials and promoting the efficiency of reducing-gas diffusion. As a result, bitumite presented a better product index compared with other reductants.

(2) The use of bitumite as reductant with a C/Fe molar ratio of 1.4 at a reduction temperature of 1200°C for 120 min resulted in DRIP assaying 90.28wt% TFe and 0.91wt% TiO_2 with an iron recovery of 91.83% and titanium concentrate assaying 46.01wt% TiO_2 with a TiO_2 recovery of 91.19%. Titanium existed mainly in the form of anosovite and ilmenite in the titanium concentrate.

(3) Embedding direct reduction is not favorable at high temperatures because of the emergence of a molten phase and iron-joined crystals during the reduction process, which in turn reduces the diffusion rate of the reducing gas and impedes the reduction reaction in the central area. In addition, some titanium-bearing minerals are enwrapped by metallic iron during the aggregation of metallic iron particles at high temperatures, which adversely affects the magnetic separation of titanium and iron.

Acknowledgement

This work was financially supported by the National Natural Science Foundation of China (Nos. 51474018 and 51674018).

References

[1] W.S. Zhang, Z.W. Zhu, and C.Y. Cheng, A literature review of titanium metallurgical processes, *Hydrometallurgy*, 108(2011), No. 3-4, p. 177.

[2] J. Deng, X. Xue, and G.G. Liu, Current situation and development of comprehensive utilization of vanadium-bearing titanomagnetite at Pangang, *J. Marer. Met.*, 6(2007), No. 2, p. 83.

[3] Y.M. Wang, Z.F. Yuan, Z.C. Guo, Q.Q. Tang, Z.Y. Li, and W.Z. Jiang, Reduction mechanism of natural ilmenite with graphite, *Trans. Nonferrous Met. Soc. China*, 18(2008), No. 4, p. 962.

[4] H.Y. Sun, J.S. Wang, X.J. Dong, and Q.G. Xue, A literature review of titanium slag metallurgical processes, *Metal. Int.*, 17(2012), No. 7, p. 49.

[5] E. Park and O. Ostrovski, Reduction of titania–ferrous ore by carbon monoxide, *ISIJ Int.*, 43(2003), No. 9, p. 1316.

[6] T.Y. Hu, T.C. Sun, J. Kou, C. Geng, X.P. Wang, and C. Chen, Recovering titanium and iron by co-reduction roasting of seaside titanomagnetite and blast furnace dust, *Int. J. Miner. Process.*, 165(2011), p. 28.

[7] Z.S. Hu, Y.S. Zhang, Y.H. Yang, X.Y. Li, and M.G. Zhou, Problems and Suggestions in the Exploitation of Beach Placer, *Multipurpose Util. Miner. Res.*, (2011), No. 4, p. 74.

[8] S.H. Wu, Reasonable utilization ways of V–Ti bearing beach placer, *Sintering Pelletizing*, 36(2011), No. 2, p. 35.

[9] B.X. Hong and W.Z. Fu, A study of the mineral composition of vanadium titanium magnetite in Indonesia, *Multipurpose Util. Miner. Res.*, (2012), No. 5, p. 44.

[10] D.S. Chen, B. Song, L.N. Wang, T. Qi, Y. Wang, and W.J. Wang, Solid state reduction of Panzhihua titanomagnetite concentrates with pulverized coal, *Miner. Eng.*, 24(2011), No. 8, p. 864.

[11] B.C. Jena, W. Dresler, and I.G. Reilly, Extraction of titanium, vanadium and iron from titanomagnetite deposits at pipestone lake, Manitoba, Canada, *Miner. Eng.*, 8(1995), No. 1-2, p. 159.

[12] K.C. Sole, Recovery of titanium from the leach liquors of titaniferous magnetites by solvent extraction: Part 1. Review of the literature and aqueous thermodynamics, *Hydrometallurgy*, 51(1999), No. 2, p. 239.

[13] K.C. Sole, Recovery of titanium from the leach liquors of titaniferous magnetites by solvent extraction: Part 2. Laboratory-scale studies, *Hydrometallurgy*, 51(1999), No. 3, p. 263.

[14] T.Y. Hu, T.C. Sun, J. Kou, C. Geng, and Y.Q. Zhao, Effects and mechanisms of fluorite on the co-reduction of blast furnace dust and seaside titanomagnetite, *Int. J. Miner. Metall. Mater.*, 24(2017), No. 11, p. 1201.

[15] E.X. Gao, T.C. Sun, C.Y. Xu, Z.G. Liu, Z.Z. Liu, and C.X. Yu, Titanium and ferrum separation of a seaside titanomagnetite based on reduction roasting, *Met. Mine*, 2013, No. 11, p. 46.

[16] C. Geng, T.C. Sun, H.F. Yang, Y.W. Ma, E.X. Gao, and C.Y. Xu, Effect of Na_2SO_4 on the embedding direct reduction of beach titanomagnetite and the separation of titanium and iron by magnetic separation, *ISIJ Int.*, 55(2015), No. 12, p. 2543

[17] E.X. Gao, T.C. Sun, Z.G. Liu, C. Geng, and C.Y. Xu, Effect of sodium sulfate on direct reduction of beach titanomagnetite for separationof iron and titanium, *J. Iron Steel Res. Int.*, 23(2016), No. 5, p. 428.

[18] M.Y. Wang, S.F. Zhou, X.W. Wang, B.F. Chen, H.X. Yang, S.K. Wang, and P.F. Luo, Recovery of Iron from chromium vanadium-bearing titanomagnetite concentrate by direct reduction, *JOM*, 68(2016), No. 10, p. 2698.

[19] G.W. Wang, J.L. Zhang, X.M. Hou, J.G. Shao, and W.W. Geng, Study on CO_2 gasification properties and kinetics of biomass chars and anthracite char, *Bioresour. Technol.*, 177(2015), p. 66.

[20] W. Lv, X.W. Lv, J.Y. Xiang, Y.Y. Zhang, S.P. Li, C.G. Bai, B. Song, and K.X. Han, A novel process to prepare high-titanium slag by carbothermic reduction of pre-oxidized ilmenite concentrate with the addition of Na_2SO_4, *Int. J. Miner. Process.*, 167(2017), p. 68.

[21] W. Yu, T.C. Sun, Q. Cui , C.Y. Xu, and J. Kou, Effect of coal type on the reduction and magnetic separation of a high-phosphorus oolitic hematite ore, *ISIJ Int.*, 55(2015), No.

3, p. 536.

[22] S.M. Jung, Thermogravimetry and reaction gas analysis of the carbothermic reduction of titanomagnetite ores with char, *ISIJ Int.*, 54(2014), No. 4, p. 781.

[23] W. Yu, *Study on the Preparation of High-phosphours Oolitic Hematite-coal Composite Briquette and Its Direct Reduction–magnetic Separation* [Dissertation], University of Science and Technology Beijing, Beijing, 2015, p. 64.

[24] Y.L. Li, T.C. Sun, J. Kou, Q. Guo, and C.Y. Xu, Study on phosphorus removal of high-phosphorus oolitic hematite by coal-based direct reduction and magnetic separation, *Miner. Process. Extr. Metall. Rev.*, 35(2014), No. 1, p. 66.